Journal of Molecular Structure 1232 (2021) 130052

Contents lists available at ScienceDirect

Journal of Molecular Structure

journal homepage: www.elsevier.com/locate/molstr

Spectroscopic evaluation of chalcone derivatives and their zinc metal complexes: A combined experimental and computational approach studying the interactions of the complexes with the serum albumin

Manos C. Vlasiou*, Amina Al Hatahta

Department of Life and Health Sciences, University of Nicosia, Nicosia 2417, Cyprus

ARTICLE INFO

Article history:
Received 2 December 2020
Revised 22 January 2021
Accepted 28 January 2021
Available online 4 February 2021

Keywords:
Chalcone
Zinc
Spectroscopy
Docking
Molecular dynamics
Complexes
DFT
HSA

ABSTRACT

Three chalcone derivatives (**L_1, L_2, L_3**) were synthesized using Claisen-Schmidt condensation reaction. Their molecular structures and spectroscopic properties (IR, UV-vis, ^{1}HNMR), were calculated at B3LYP level. Electrostatic interactions and HOMO-LUMO properties were calculated using TD-DFT method. Molecular docking was used to compare the HSA (human serum albumin) interactions with the ligands and their Zn complexes (**C_1, C_2, C_3**) which were synthesized by interaction between the ligands and the Zn (II) ion in a 2:1 M ratio. Elemental analysis, FT-IR, and UV–Vis spectroscopy studies investigated the structure of the synthesized complexes. UV–Vis, molecular docking and molecular dynamics were used to study the interactions of the Zn complexes with the BSA (bovine serum albumin). The biological activity of the Zn-Chalcone complexes was generally higher than the chalcones when evaluated spectroscopically and theoretically.

1. Introduction

Chalcones, are belonging to the flavonoid family, having a medicinal importance because of the CO-CH=CH- (ketoethylenic group). There are intermediates of flavonoids and they exhibit anti-inflammatory, antifungal, antimicrobial, antioxidant and anti-tumor activity [1,2]. This biological activity is because of the α, β-unsaturated keto function. Chalcone contains two aromatic rings linked by a three carbon α, β-unsaturated carbonic system and they are selected because of their low toxicity and possible chemical modification [3,4]. In nature, chalcone (1,3-diphenyl-2-propen-1-one) is one of the open chain flavonoids containing 15-carbon arranged in a C6C3-C6 configuration [5]. The bioactivity of chalcones have been studied and several biological activities have been found such as, antioxidant, cytotoxic, antiviral, tyrosinase inhibitory, antimalarial, antibacterial, and anti-inflammatory [6]. Additionally, the synthesis of Pd (II) and Pt (II) complexes and Co (II), Cu (II), Mn (III) of a chalcone compound has been proposed elsewhere [7,8] and this is because chalcones are effective metal ion chelators and they can easily create metal-coordinated compounds [9]. Chalcones are synthesized by Claisen–Schmidt condensation. This reaction involves cross aldol condensation of appropriate aldehydes and ketones by base catalysed or acid catalysed reactions followed by dehydration [10].

It is known that Zinc-containing compounds play a key role in carbonic anhydrases, peptidases, proteases, and deaminases [11]. Interestingly, the coordination chemistry of zinc in proteins and peptides involves N, O, and S donors of the side chains of histidine, glutamate/aspartate, and/or cysteine with any permutation of these ligands and with the number of protein ligands ranging from three to six [12]. On the other hand, Zn plays a vital role in a variety of biological processes but, excessive exposure of Zn^{2+} to human beings can cause toxicity, inducing a series of overt poisoning symptoms and neurodegenerative disorders [13].

HSA is responsible to maintaining stable osmotic pressure and to carrying endogenous or exogenous compounds. Additionally, most lipophilic drugs are substrates of HSA and are transferred to target tissues via the bloodstream. The chemical structure of HSA includes three homologous α-helical domains (I, II and III), each of which possesses two subdomains (A and B) [14]. Various binding and denaturation studies have shown to be a rapid and effective tool for the characterization of albumin binding sites and their enantioselectivity, and for the study of the changes in the binding properties of the protein caused by interaction between different ligands [15-18].

* Corresponding author.
E-mail address: vlasiou.m@unic.ac.cy (M.C. Vlasiou).

https://doi.org/10.1016/j.molstruc.2021.130052
0022-2860/

The last years more and more scientists are using computational chemistry and theoretical tools to evaluate their molecular structures [19-21]. Moreover, some researchers are using computational tools to evaluate the biological activity of the molecules of interest [22-26]. This is because of the quick results that the computational tool is giving to the researcher, and the added scientific value to the findings. All that, at minimum cost and resources. As the technological improvements are running fast, more and more theoretical tools are going to save time to the researcher and give a different perspective, using the predictive character of the computerized models.

Herein, we propose the synthesis of some chalcone analogues, and their complexation with Zn (II) metal ions. In total, 6 molecules were prepared and evaluated spectroscopically, both *in situ* and theoretically. More specifically, we used TD-DFT studies [26-31], to evaluate our chalcone derivatives in terms of structure and activity, molecular docking [32-35], to evaluate their interaction with human serum albumin (HSA) and spectroscopy to evaluate their binding interactions with bovine serum albumin (BSA). The biological activity of the chalcone derivatives, was compared with the biological activity of their counter Zn complexes.

2. Experimental

2.1. Materials

2-nitrobenzaldehyde, 2-(methylamino) benzaldehyde, 2-hydroxy-5-methylphenyl ethanone, 1-(2-hydroxy-5-methylphenyl) ethanone, 4-hydroxy-3-methoxyphenyl ethanone, were purchased from Merck. Solvents were used without any further purification. Other reagents were of analytical grade. BSA (bovine serum albumin) (purity $\geq$ 98%) was purchased from Merck.

2.2. Instruments

All the chalcone analogues and their zinc complexes were characterized by ^{1}HNMR, recorded on Bruker 300 MHz spectrometer using DMSO-d6 as solvent and TMS as an internal standard. The chemical shifts were expressed in δ ppm. The absorption spectrum of all the reaction mixtures was then taken in a range of 200-400 nm in a JASCO (Tokyo, Japan) UV-visible spectrophotometer using a 1cm path length quartz cuvette.

2.3. Synthesis of chalcones analogues

2.3.1. Synthesis of (E)-1-(2-hydroxy-5-methylphenyl)-3-(2-nitrophenyl) prop-2-en-1-one

In a round bottom flask (100 ml), to a methanolic solution (20 ml) of 2-hydroxy-5-methylphenyl ethanone (0.003 mol) a 40% aqueous NaOH solution (15 mL) was gradually added. 2-nitrobenzaldehyde (0.003 mol) was added and the reaction took place for 20 h at 25°C. Any precipitate formed was removed by filtration and the filtrate was acidified with dilute HCl and then extracted with chloroform. The concentrate of the chloroform was chromatographed over silica gel to obtain the desired product. The compound then crystallized from chloroform-petroleum ether (50:50). Olive green solid, M.P: 55-57 º C; ^{1}H NMR (300 MHz, DMSO-d6): δ 2.36 (s,-CH_3), 5.37 (s, -OH), 7.04 (m, -CH aromatic), 7.36 (m, -CH aromatic), 7.44 (m, -CH aromatic), 7.65 (m, -H), 7.89 (m, -CH), 8.23 (m, -CH), 8.64 (m. -H) *ppm*.

2.3.2. Synthesis of (E)-3-(4-dimethylamino) phenyl)-1-(2-hydroxy-5-methylphenyl) prop-2-en-1-one

In a round bottom flask (100 ml), to a methanolic solution (20 ml) of 2-hydroxy-5-methylphenyl ethanone (0.003 mol) a 40% aqueous NaOH solution (15 mL) was gradually added. 4-dimethylamino benzaldehyde (0.003 mol) was added and the reaction took place for 20 h at 25°C. Any precipitate formed was removed by filtration and the filtrate was acidified with dilute HCl and then extracted with chloroform. Orange solid, M. P: 54-55 ° C; ^{1}H NMR (300 MHz, DMSO-d6): δ 2.34 (s, -CH_3), 3.06 (s, -CH_3), 5.35 (s, -OH), 7.02 (m, -CH aromatic), 7.34 (m, -CH aromatic), 8.33 (d, -H) *ppm*.

2.3.3. Synthesis of (E)-1-(2-hydroxy-5methoxyphenyl)-3-(2-nitrophenyl) prop-2-en-1-one

In a round bottom flask (100 ml), to an ethanolic solution (20 ml) of 1-(4-hydroxy-3methoxyphenyl) ethanone 0.003 mol) a 40% aqueous NaOH solution (20 mL) was gradually added. 2-nitrobenzaldehyde (0.003 mol) was added and the reaction took place for 24 h at 25°C. Any precipitate formed was removed by filtration and the filtrate was acidified with dilute HCl. Yellow-green solid, M. P: 57-59 ° C; ^{1}H NMR (300 MHz, DMSO-d6): δ 3.84 (s, -CH3), 5.33 (s, -OH), 7.10 (m, -CH aromatic), 7.27 (m, -CH aromatic), 7.79 (m, -CH aromatic), 7.89 (m, -CH aromatic), 8.21 (m, -CH aromatic), 8.60 (d, -H).

2.4. Synthesis of Zinc (II) Complexes

Zn (II) complexes with ligands L_1-L_3

An ethanolic solution (30 ml) of Zn (II) chloride (0.01 mol) was added to a refluxing solution of appropriate chalcone analogue L_1-L_3 (0.02 mol) in ethanol (30 ml). The reaction mixture was refluxed for 6 h. The coloured complexes were obtained, filtered off, washed with ethanol and dried under vacuum. Elemental Analysis: L1: C, 54.84; H, 3.45; Cl, 10.12; N, 4.00; O, 18.26; Zn, 9.33. L2: C, 62.04; H, 5.21; Cl, 10.17; N, 4.02; O, 9.18; Zn, 9.38. L3: C, 52.45; H, 3.30; Cl, 9.68; N, 3.82; O, 21.83; Zn, 8.92. Molar Conductance (M hos.cm^2 mol^{-1}): C_1: 12.03, C_2: 12.09, C_3: 11.99.

2.5. Theoretical Studies

2.5.1. Optimization and vibration frequency calculations were made at B3LYP level with ORCA version 4.0.1 program

B3LYP is a hybrid density functional theory method. Among the ever-increasing number of DFT methods, the hybrid functional B3LYP, as a good compromise between computational cost, coverage, and accuracy of results [36]. It has become a standard method used to study organic chemistry in the gas phase. UV-vis spectrums at the same level calculated by time-dependent density functional theory (TD-DFT) method. ORCA input files were created by AVOGADRO version 1.2.0 software. HOMO energy (E_{HOMO}) and LUMO energy (E_{LUMO}) were taken from the output file. Chalcone analogues and their zinc complexes were docked against human serum albumin. Molecular docking studies were carried out by using iGEMDOCK 2.1 software [11]. The HSA coded crystal structure was selected from the Protein Data Bank (www.rcsb.org). The population size was = 200, generations = 70, number of solutions = 3.

2.6. Effect of the ligand and the complex on the absorption spectrum of BSA

The effect of the ligands and their corresponding complexes, on the absorption spectrum of BSA, was studied using UV–visible spectrophotometry. Briefly, BSA (5 μM) were incubated in the absence and presence of 2-9 μM of L_1, L_2, L_3, C_1, C_2 and C_3 for 30 min at RT.

2.7. Conductance studies on the Zn-complexes interaction with BSA

All stock solutions were prepared freshly by weighing and using freshly prepared solvents. Conductivity measurements were made

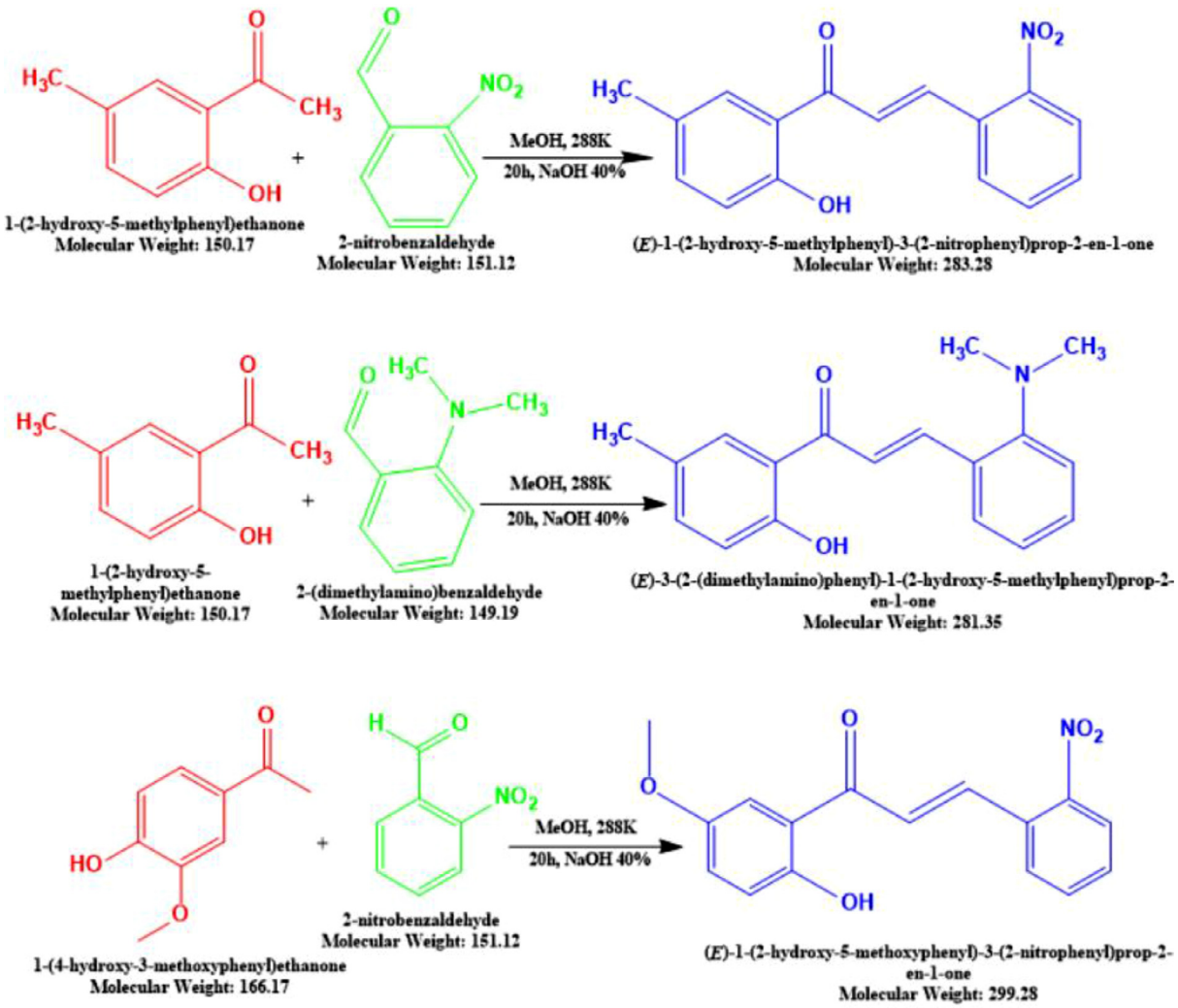

Fig. 1. Synthetic routes of the three chalcone derivatives.

using EC/TEMP meter AD 130 model at room temperature. A standard addition method has been used for measuring the conductance of the ligand-protein complexes. BSA (5 μM) was left to react with different concentrations of the C_1, C_2, C_3 molecules. A certain amount of solution was injected into the conductivity cell and the conductivity of the solution was measured. 10 additions have been made throughout.

3. Results and discussion

Synthesis of Chalcone Derivatives and their Zinc Complexes

Chalcone derivatives were synthesized based on Claisen-Schmidt condensation reaction. Acetophenones analogues reacted in (1:1) ratio with benzaldehydes analogues in methanolic solutions resulting the chalcone derivatives (**L_1, L_2** and **L_3**). The synthetic routes and conditions are depicted in Fig. 1. Reactions took place at room temperature resulting colourful precipitates after 20 h mixing. Any precipitate formed was removed by filtration before acidification. The formation of carbanion or enolate ions is considered to be the first stage of the condensation reaction. Aromatic ketones having α hydrogen if treated with alkaline solutions (in this case NaOH), the hydroxide ion from the base will attack hydrogen α from the ketone so that a carbanion is formed which can be stabilized by resonance and release the H_2O molecule. Followed by the second stage which is a nucleophilic addition reaction. Here, the enolate or carbanion ion formed at stage one acts as a nucleophile that attacks the carbonyl group of benzaldehyde. An alkoxide ion is formed which has an excess of electron charge in the O atom. Next, is the formation of an aldol. Aldol is a compound formed from aldehydes and ketones where aldol takes protons from solvent molecules, H_2O. Alkoxide ions take hydrogen protons from H_2O molecules to form β-hydroxyketone (aldol). Then the hydroxide ion from H_2O binds to the sodium ion and returns to form a NaOH base catalyst. Finally, the dehydration reaction of the aldol compound takes place in Claisen-Schmidt reaction. Dehydration reaction is a reaction of the release of water molecules. Carbonyl β-hydroxy like aldol is easily dehydrated, because the double bonds in the compound conjugate with the carbonyl group. The disappearance of the chemical shift at 2.5 ppm attributed to -CH_3 hydrogens of acetophenone, it is a good evidence of the resulted chalcone derivatives. Moreover, the increase of the melting points from 47°C to 57°C is another indicator of the successful synthesis.

Zn (II) complexes (**C_1, C_2** and **C_3**) resulted after mixing ethanolic chalcone derivative solution (L_1, L_2 and L_3) with $ZnCl_2$ at (1:2) ratio, using reflux for 6 h. Coloured complexes obtained after filtration. The three complexes are soluble to DMSO and DMF. Elemental analyser indicated that the complexes have 1:2 metal to ligands stoichiometry of the types $[ZnL_2(Cl)_2]$, whereas L are the chalcone

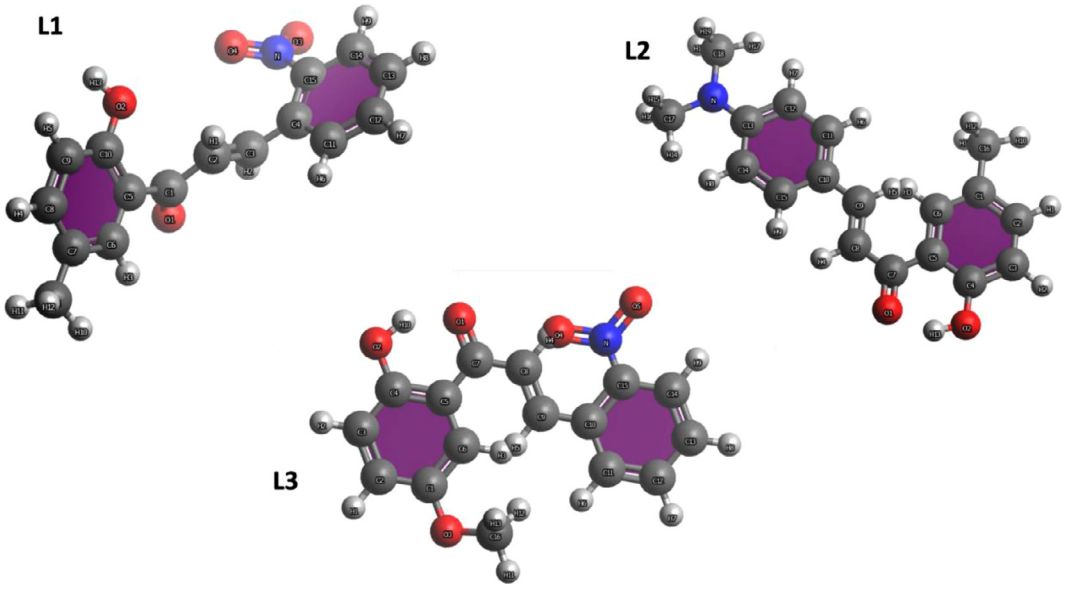

Fig. 2. Optimized structures of the synthesized chalcones.

Table 1
Selected bond lengths (Å) and bond angles (°) of the synthesized chalcones.

L1	Atoms	Angle	Atoms	Length
	C5-C1-O1	119.2789	H4-C8	1.08865
	C2-C1-C5	118.1423	C8-C9	1.40054
	C1-C7-H1	118.5631	H13-O2	0.972961
	C14-C15-N	122.4757	C10-O2	1.36579
	H10-C16-H12	107.4257	O4-N	1.23645
	C10-O2-H13	109.1858	N-C15	1.47324
	O3-N-O4	123.7386		
	C15-N-O4	119.113		
L2	C2-C1-C6	120.0083	H15-C17	1.11298
	C1-C2-H1	120.0048	C17-N	1.47004
	C5-C4-O2	120.0014	C12-C11	1.3949
	C12-C13-N	119.9951	C7-O1	1.20804
	H10-C16-H12	109.4628	H13-O2	0.97205
	C4-O2-H13	108.0009		
	C17-N-C18	119.9963		
	N-C17-H15	109.4457		
L3	C2-C1-C6	119.9986	H13-C16	1.11302
	C2-C1-O3	120.0016	C16-O3	1.40206
	C3-C2-H1	120.033	C13-C14	1.39477
	C14-C15-N	119.9599	O5-N	1.31001
	C4-O2-H10	107.9991	C15-N	1.24809
	C1-O3-C16	110.8014	H10-O2	0.971976
	H12-C16-H13	109.5253		
	O3-C16-H11	109.4976		
	C15-N-O4	120.004		

derivatives resulted after the condensation of the correct acetophenone analogue with the correct benzaldehyde analogue. In addition, low molar conductance values indicate that the complexes are not electrolytes.

Theoretical Studies on Chalcone Derivatives

Molecular Geometry

The ground state optimization structures of the synthesized chalcone molecules were obtained in the aqueous phase at B3LYP def2-TZVP Grid5 level and are given in Fig. 2.

The geometrical parameters have been procured from optimized molecular structure and summarized in Table 1, giving the main theoretically calculated bond lengths and bond angles of the molecules.

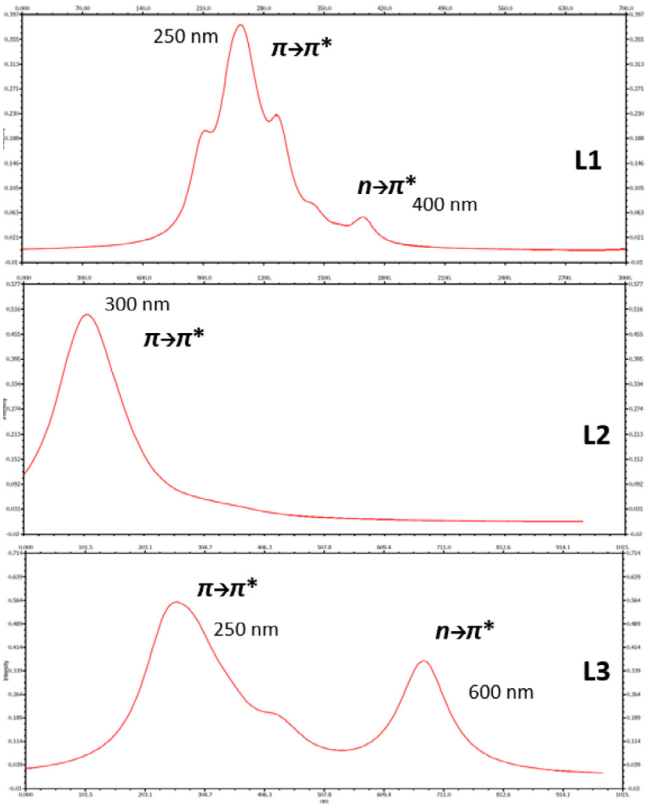

Fig. 3. Calculated UV-vis spectra of **L1, L2** and **L3** molecules.

Spectroscopy

The spectroscopic UV-vis spectrum of the three ligand molecules, and their electronic transitions can be computerized and analyzed by time-depended density functional theory or TD-DFT. Additional information in the molecular structure prediction can be taken by electronic spectroscopy. In Fig. 3 we can see the

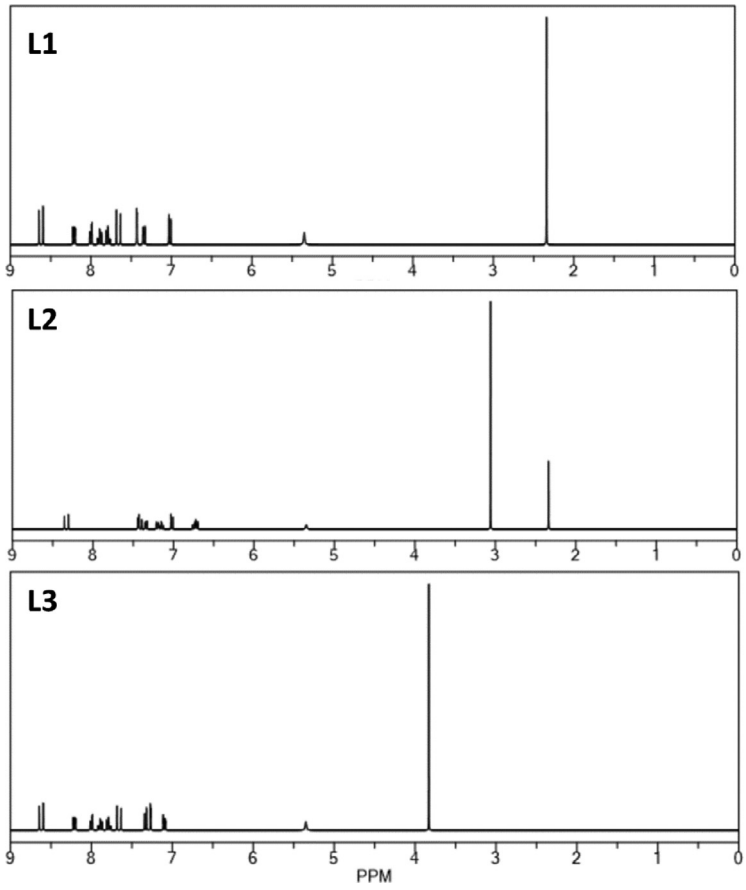

Fig. 4. Calculated ^{1}HNMR spectra of $\mathbf{L_1}$, $\mathbf{L_2}$ and $\mathbf{L_3}$ molecules.

calculated UV-vis spectrum of the molecules taken in the aqueous phase using B3LYP def2-TZVP Grid5 level algorithm.

As seen in **Fig. 3**, for $\mathbf{L_1}$ and $\mathbf{L_3}$ are observed similar spectrums giving two bands for $\boldsymbol{\pi \rightarrow \pi^*}$ and $\boldsymbol{n \rightarrow \pi^*}$ transitions respectively. Most absorption spectroscopy of organic compounds is based on transitions of n or π electrons to the π^* excited state [37]. This is because the absorption peaks for these transitions fall in an experimentally convenient region of the spectrum (200 - 700 nm). These transitions need an unsaturated group in the molecule to provide the π electrons. For $\mathbf{L_2}$ molecule only one transition is observed the $\boldsymbol{\pi \rightarrow \pi^*}$**.** The similarity of the bands shapes and close wavelengths show that the structures of the studied molecules are quite similar as they are belonging to the same family of the chalcones. ^{1}HNMR spectrum calculated data also suggest the similarity of the structures.

For structural characterization ^{1}HNMR spectra of chalcone molecules were calculated and peaks were attributed to the correct chemical groups. Chemical shifts were given according to the TMS reference and calculated from $\delta = \Sigma_{TMS} - \Sigma_{relation}$, whereas Σ_{TMS} corresponds to the shielding of proton to the TMS and Σ, the shielding of proton in the sample. The ^{1}HNMR spectrum calculated at B3LYP DEF2-TZVPP DEF2 level in aqueous phase and are given in Fig. 4.

Chemical shifts of ^{1}HNMR, are given in Table 2.

As can be seen in Fig. 4, the spectra are similar for molecules $\mathbf{L_1}$, $\mathbf{L_3}$ same as the UV-vis spectra. The only difference is the shift of the first chemical shift from 3.83 to 2.34 ppm due to the presence of the extra methyl group on $\mathbf{L_3}$. The presence of the 3.06 ppm chemical shift that it is characteristic for the $\mathbf{L_2}$ and corresponds to the -CH_3 group of the molecule, dominates the anomeric region. Because they are attached to carbon atoms with low *s*-character

Table 2
^{1}HNMR chemical shifts of chalcone molecules calculated at aqueous phase.

L1		L2		L3	
Group	**Shift (ppm)**	**Group**	**Shift (ppm)**	**Group**	**Shift (ppm)**
OH	5.35	**OH**	5.35	**OH**	5.35
CH	7.02	**CH**	7.02	**CH**	7.1
CH	8.21	**CH**	6.71	**CH**	7.33
CH	7.43	**CH**	7.43	**CH**	8.21
CH	8	**CH**	7.2	**CH**	7.27
CH	7.34	**CH**	7.34	**CH**	8
CH	7.89	**CH**	7.15	**CH**	7.89
CH	7.79	**CH**	6.74	**CH**	7.89
CH_3	2.34	**CH_3**	3.06	**CH_3**	3.83
H	8.02	**CH_3**	3.06	**H**	8.62
H	7.66	**CH_3**	2.34	**H**	7.66
		H	8.33		
		H	7.42		

hybridization (sp^3) the found in a low ppm chemical shift. The aromatic region of the spectra of the three chalcone derivatives are quite similar. As can be seen from Table 2**.** the -OH group is present at three molecules as well, at the same chemical shift 5.35 ppm. The hydrogens of the phenol group of the chalcones can be found at 8.02 and 7.66 ppm for $\mathbf{L_1}$, 8.33 and 7.42 ppm for $\mathbf{L_2}$**,** and 8.62 and 7.66 ppm for $\mathbf{L_3}$.

An additional way to verify the structures of the chalcone derivatives, is the vibrational spectrum. It has been calculated by BP86 DEF2-SVP FREQ algorithm. The high intensity peaks with the harmonic vibration frequencies are given in Fig. 5.

The characteristic high frequency peak at 3500 cm^{-1}, of s(O-H) is common for the three analogues, while the peak at 1200 cm^{-1} for $\mathbf{L_1}$, indicating the s(N-H) vibration. The methoxy group of $\mathbf{L_3}$,

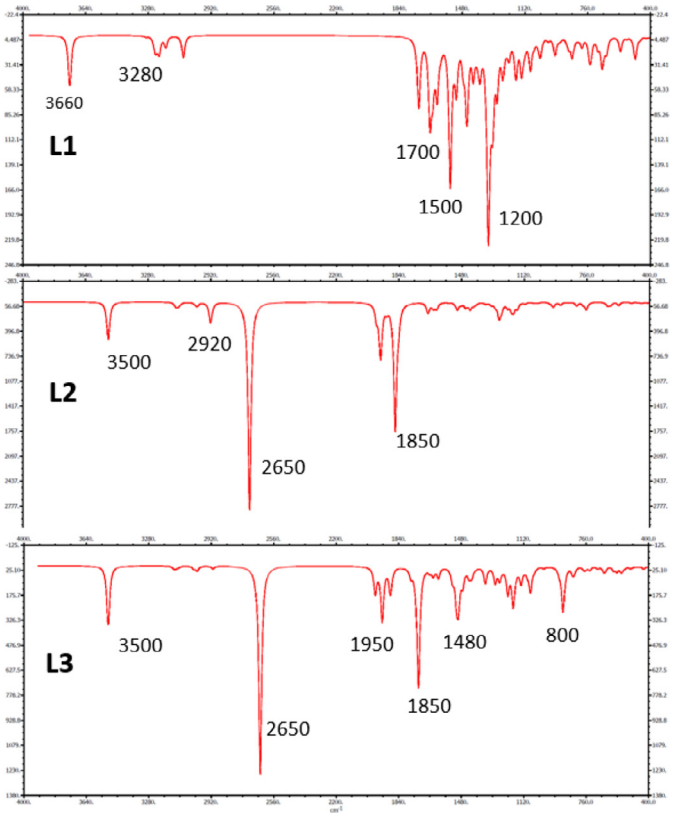

Fig. 5. IR spectra of $\mathbf{L_1}$, $\mathbf{L_2}$ and $\mathbf{L_3}$ chalcone derivatives calculated in aqueous phase.

is responsible for the t(H-O-C-C) vibration at 800cm^{-1} which is absent for $\mathbf{L_1}$ and $\mathbf{L_2}$. The 1700 cm-1 peak is responsible for the s(N-C) of the molecules, while the 1500 cm^{-1} peak is responsible for s(N-O) that is why it is absent from $\mathbf{L_2}$ [38].

Molecular Orbital Studies

The molecular orbital studies revealed the energy gap between the highest molecular orbital (HOMO) and the lowest molecular orbital (LUMO). The value of the energy difference between HOMO and LUMO as well as the highest occupied molecular orbital (EHOMO) and lowest unoccupied molecular orbital (ELUMO) energies plays a very important role in stability and reactivity of molecules. The EHOMO energies of molecules show the molecule's ability to give electrons. On the other hand, ELUMO characterizes the ability of the compound to accept electrons [38]. Thus, the one is nucleophile and the other electrophile. Molecules with small energy gaps are considering to have a higher chemical reactivity and softer structures, while molecules having larger energy gaps are considering to be more stable and chemically harder. The computed values of the three chalcone derivatives can be found in Fig. 6.

Table 3
Calculated energy values of the molecules.

Molecule	L1	L2	L3
Potential Energy (Kcal/mol)	-2.015	-1.871	-2.175
Kinetic Energy (Kcal/mol)	1.003	9.317	1.089
Magnitute (a.u)	2.202	3.991	2.326
Zero Point Energy (Kcal/mol)	157.90	215.90	237.07
Total Thermal Energy (Kcal/mol)	-1.013	-9.385	-1.085
Total Enthalpy (Kcal/mol)	-1.013	-9.385	-1.085
Final Entropy (Kcal/mol)	37.09	33.74	33.11
Gibbs Free Energy (Kcal/mol)	-1.013	-9.386	-1.085
E_{Lumo} (eV)	-1.817	0.58	-4.259
E_{Homo} (eV)	-4.057	-1.757	-4.646
Δ_E (eV)	2.24	2.34	0.38

It seems that $\mathbf{L_3}$, has the highest reactivity (ΔE= 0.38 *eV*) followed by $\mathbf{L_1}$ (ΔE= 2.24 *eV*) and $\mathbf{L_2}$ (ΔE= 2.34 *eV*). In Table 3. we can see all the calculated energy features of the three molecules including, enthalpy, entropy and Gibbs energy. Any process in which the number of particles in the system increases consequently results in an increase in disorder. This is why we can observe an increase in the entropy of the molecules.

The individual charge on each atom on the molecule, it is another factor used to characterised molecular structures and it is presented by the Mulliken population study [39]. The Mulliken atomic charges have been calculated by DFT method and presented in Table 4.

The O20 atom has the highest negative charge for $\mathbf{L_1}$, while for $\mathbf{L_2}$ the highest negative charge belongs to C2 atom. For $\mathbf{L_3}$ the highest negative charge is that of C2 atom as well. On the other hand, N18 and H33 atoms are having the highest electropositive charge

Table 4
Calculated Mulliken atomic structures of the synthesised structures.

		L1		L2		L3			L1		L2		L3
0	C	0.063637	C	0.129145	C	0.196881	**21**	H	0.016168	H	-0.12029	O	-0.45753
1	C	-0.01498	C	-0.06418	C	-0.16668	**22**	H	0.055123	H	-0.66633	H	0.121061
2	C	0.006626	C	**-2.15955**	C	**-0.20199**	**23**	H	-0.0143	H	0.131908	H	0.126387
3	C	0.005301	C	0.145811	C	**0.216942**	**24**	H	-0.01752	H	0.111987	H	0.174554
4	C	-0.01552	C	0.086392	C	-0.01596	**25**	H	-0.02783	H	0.120226	H	-0.809
5	O	-0.18649	O	-0.37377	C	0.011232	**26**	H	0.007255	H	0.092538	H	-0.40756
6	C	-0.03756	C	-0.31097	C	0.186225	**27**	H	0.011455	H	0.086498	H	0.08526
7	C	-0.03731	C	**0.221231**	C	-0.19805	**28**	H	0.011051	H	0.0899	H	0.108883
8	C	-0.01681	C	-0.14285	C	0.219312	**29**	H	0.018982	H	0.08746	H	0.124392
9	C	-0.07558	C	-0.21923	C	-0.06535	**30**	H	0.023503	H	0.116634	H	0.152466
10	C	0.139354	C	0.108108	C	-0.1448	**31**	H	0.048161	H	0.116973	H	**0.341468**
11	C	-0.02794	C	-0.26177	C	-0.15484	**32**	H	0.034461	H	0.116384	H	0.134882
12	C	0.039388	C	-0.11634	C	-0.05795	**33**	H	**0.185554**	H	**1.869932**	H	0.100239
13	C	0.010727	C	-0.15529	C	-0.17958	**34**			H	0.176557	H	0.13827
14	C	-0.03116	C	-0.17493	C	0.081493	**35**			H	0.078148		
15	C	0.178551	C	0.023324	O	-0.40831	**36**			H	**0.219539**		
16	C	0.037741	N	-0.11198	O	-0.38967	**37**			H	0.141291		
17	O	-0.16188	C	-0.3699	O	-0.26285	**38**			H	0.111857		
18	N	**0.184202**	O	0.922754	C	-0.17764	**39**			H	0.125495		
19	O	-0.21708	C	0.07014	N	**0.220938**							
20	O	**-0.19531**	C	-0.25285	O	1.356872							

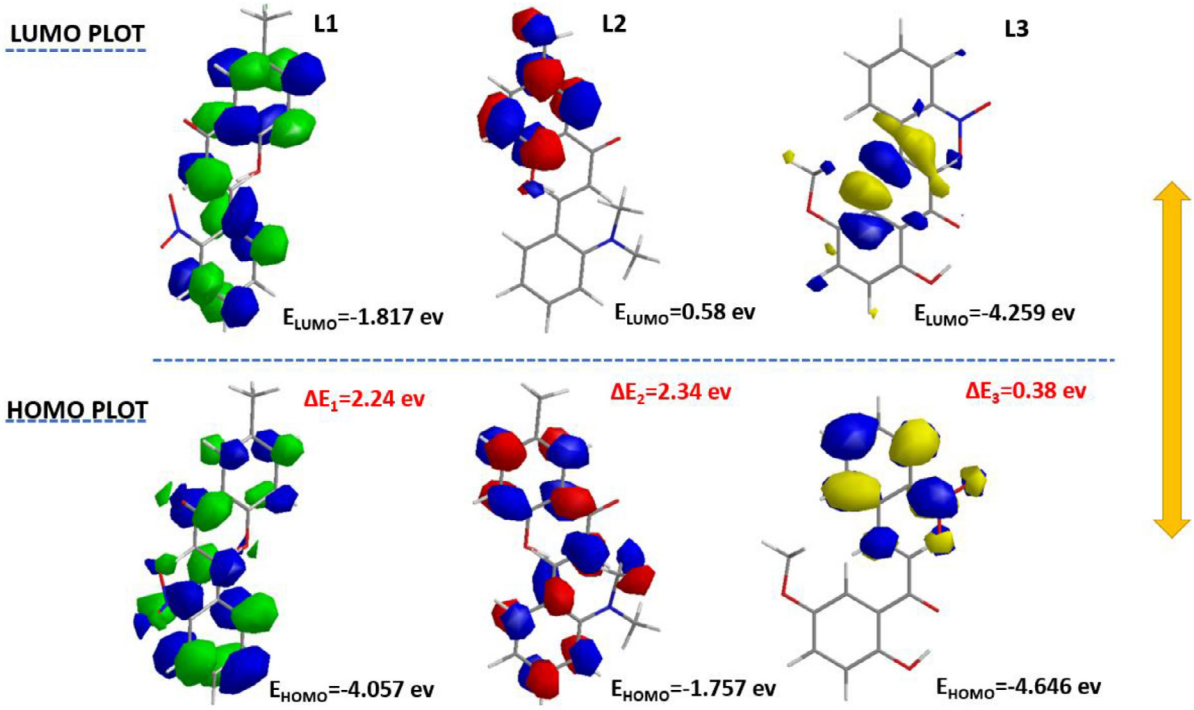

Fig. 6. HOMO-LUMO orbitals of $\mathbf{L_1}$, $\mathbf{L_2}$ and $\mathbf{L_3}$ molecules.

Table 5
Interaction types of the chalcone molecules and their zinc complexes.

Molecule	Energy (Kcal/mol)	Van der Waals (Kcal/mol)	Hydrogen Bonding (Kcal/mol)	Electrostatic Forces (Kcal/mol)
L1	-78.63	-65.08	-13.55	0
L2	-76.66	-59.16	-17.50	0
L3	-84.53	-65.31	-19.22	0
C1	-82.64	-62.09	-20.55	0
C2	-118.05	-102.97	-15.08	0
C3	-94.29	-73.61	-20.67	0

for $\mathbf{L_1}$, and C7 and H33 atoms the highest electropositive charge for $\mathbf{L_2}$. Finally, for $\mathbf{L_3}$, C3, N19 and H31 are the most electropositive atoms. The negative charges are due to the electron withdrawing groups that the atoms are attached with and the positive charges are because of the negative charges of the adjacent groups.

Biological Evaluation of Chalcone Derivatives and their Zinc Complexes

Molecular Docking

The examination of the biological activity of the three ligand molecules ($\mathbf{L_1}$, $\mathbf{L_2}$, $\mathbf{L_3}$) and their corresponding complexes ($\mathbf{C_1}$, $\mathbf{C_2}$, $\mathbf{C_3}$), calculated theoretically by molecular docking studies. Using this technique, we can predict the best drug candidate in terms of protein inhibition, on a specific targeted protein. By molecular docking, we can predict binding energies, types of interactions and the amino acid profile residue of the protein that interacts with the drug molecule. In this study, we investigated the binding affinity of our studied molecules with HSA (human serum albumin). HSA, is the main transport protein in human organisms, were drugs bind and transported throughout the blood transportation. The interaction types between the chalcone molecules and their zinc complexes are given in Table 5. The energy function can be dissected into the following terms:

$$E_{tot}=E_{bind}+E_{pharma}+E_{ligpre} \quad (1)$$

Table 6
Interactions formed between the studied molecules with the amino acids of the transport protein.

Molecule	Amino Acid Residue
L1	Hydrophilic: GLN 33 (-2.5), THR 83 (-8.5) TYR 84 (-2.5) Hydrophobic: LEU 31 (-4.8), ARG 81 (-4.1) GLU 82 (-9.6) THR 83 (-5.4)
L2	Hydrophilic: TYR 140 (-4.1) GLU 141 (-3.5) ARG 144 (-9.9) Hydrophobic: PRO 35 (-6.9) PHE 36 (-5) GLU 37 (-5) TYR 140 (-9.3)
L3	Hydrophilic: ASP 38 (-2.5) HIS 39 (-5.6) ARG 81 (-3.4) THR 83 (-6) Hydrophobic: LEU 31(-2.5) HIS 39 (-5.6) ARG 81 (-3.4) THR 83 (-6) LEU 31 (-4.3) GLN 33 (-6.1) PRO 35 (-6.4) ASP 38 (-4.4) VAL 77 (-4.5) ARG 81 (-7) TYR 84 (-4)
C1	Hydrophilic: ASP 38 (-11) THR 83 (-6.7) ARG 144 (-2.8) Hydrophobic: GLN 33 (-9.3) ASP 38 (-5.8) ARG 81 (6.3) LAU 112 (-4.9) ARG 144 (-5.1)
C2	Hydrophilic: GLN 33 (-3.2) PHE 36 (-3.1) TYR 140 (-5) ARG 144 (-3.9) Hydrophobic: GLN 33 (-7.4) PRO 35 (-9) PHE 36 (-6.1) GLU 37 (-7.7) LEU 112 (-4) TYR 140 (-13.6)
C3	Hydrophilic: ASP 38 (-10.7) ARG 81 (-8.6) Hydrophobic: GLN 33 (-11.8) PRO 35 (-7.7) ARG 81 (-11.9) THR 83 (-12.8)

where E_{bind} is the empirical binding energy used during the molecular docking; E_{pharma} is the energy of binding-site pharmacophores; and E_{ligpre} is a penalty value if the ligand unsatisfied the

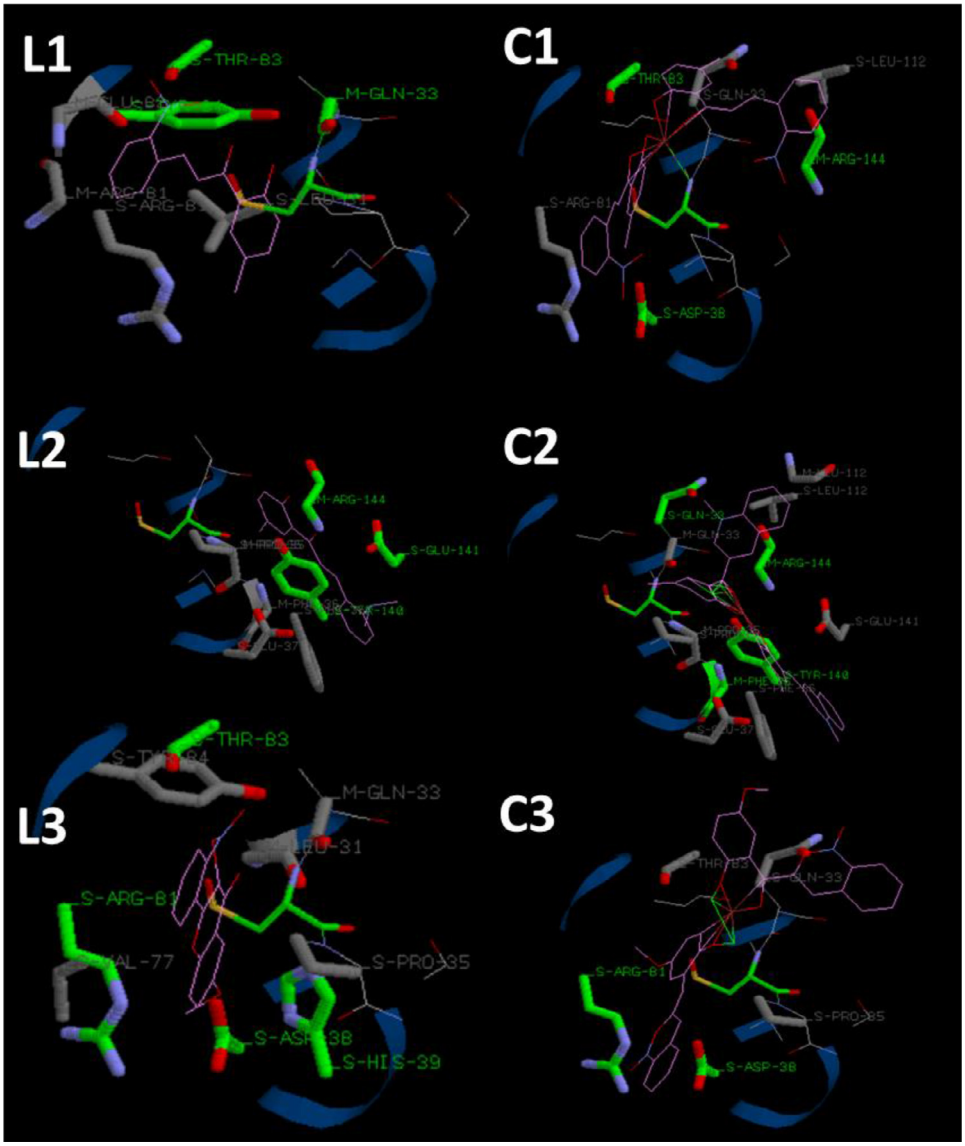

Fig. 7. Interactions of the studied molecules in human serum albumin.

ligand preferences. E_{pharma} and E_{ligpre} were used to improve the number of true positives by discriminating active compounds from hundreds of thousands of non-active compounds.

It can be seen that $\mathbf{C_2}$, exhibit the highest binding affinity on the transport protein, followed by $\mathbf{C_3}$ and $\mathbf{L_3}$. The highest binding affinity exhibited by $\mathbf{C_2}$ is because of the CH_3-N-CH_3 group which seems to interact better with the protein with van der Waals forces. The lowest binding affinity exhibited by $\mathbf{L_2}$, which means that in general, the complexed zinc (II) molecules are more active molecules with only exception the $\mathbf{C_1}$. In Table 6. the amino acid residue of the protein that interact with the studied molecules can be seen.

The best drug candidate of the six studied molecules with molecular docking ($\mathbf{C_2}$), interacts both with hydrophilic and hydrophobic interactions. More specifically, $\mathbf{C_2}$ exhibits hydrogen bonds with GLN 33, PHE 36, TYR 140 and ARG 144 amino acids. Additionally, $\mathbf{C_2}$, exhibits van der Waals interactions with GLN 33, PRO 35, PHE 36, GLU 37, LEU 112 and TYR 140 amino acids. Docking poses are depicted in Fig. 7.

BSA Binding

The structural changes of the protein and the complexation with the studied molecules has been done using UV-vis absorption measurements. The compounds interacted on the site I of the protein. We performed binding studies on the BSA protein because it has a similar shape with the HSA. The UV-vis absorption spectrums in Fig. 8 shows the effect of L_1, L_2, L_3, C_1, C_2 and C_3 molecules on the BSA spectrum. Strong absorption peaks at 250 nm and 350 nm can be seen for L_1, L_2, L_3 which are increased in intensities as the concentration of the molecules increases. The red shift observed at 250-255 nm indicates the complex formation of the protein with the ligands. When the L_1, L_2 and L_3 complexed with Zn (II), we observe in the spectrum of the protein only one strong absorption peak at 210-220 nm depending on the complex molecule. Again, the red shift of 1-5 nm corresponds to the ligation of the molecules in the protein structure. The Zn (II) ions are responsible for the loosening and unfolding of the protein backbone with an increase of the hydrophobicity of its environment, more drastically than the of L_1, L_2, L_3 molecules which Zn is absent [40]. Thus, the

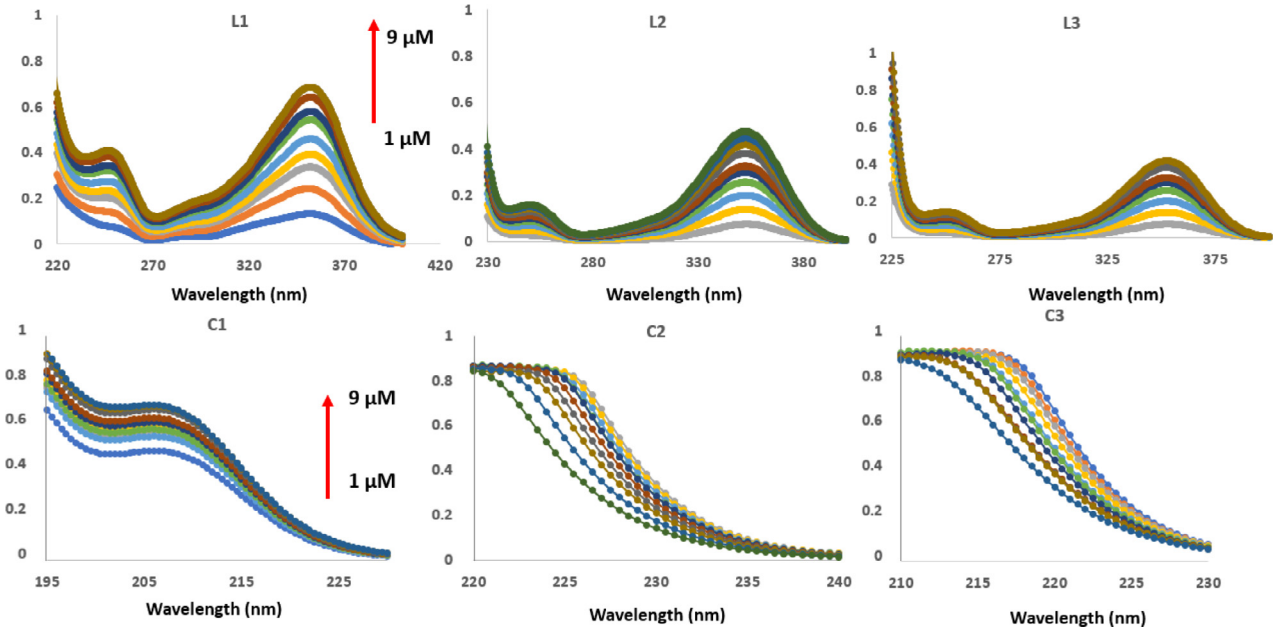

Fig. 8. UV-vis spectra of L_1, L_2, L_3, C_1, C_2, C_3 (1-9 μM) interactions with BSA (5 μM).

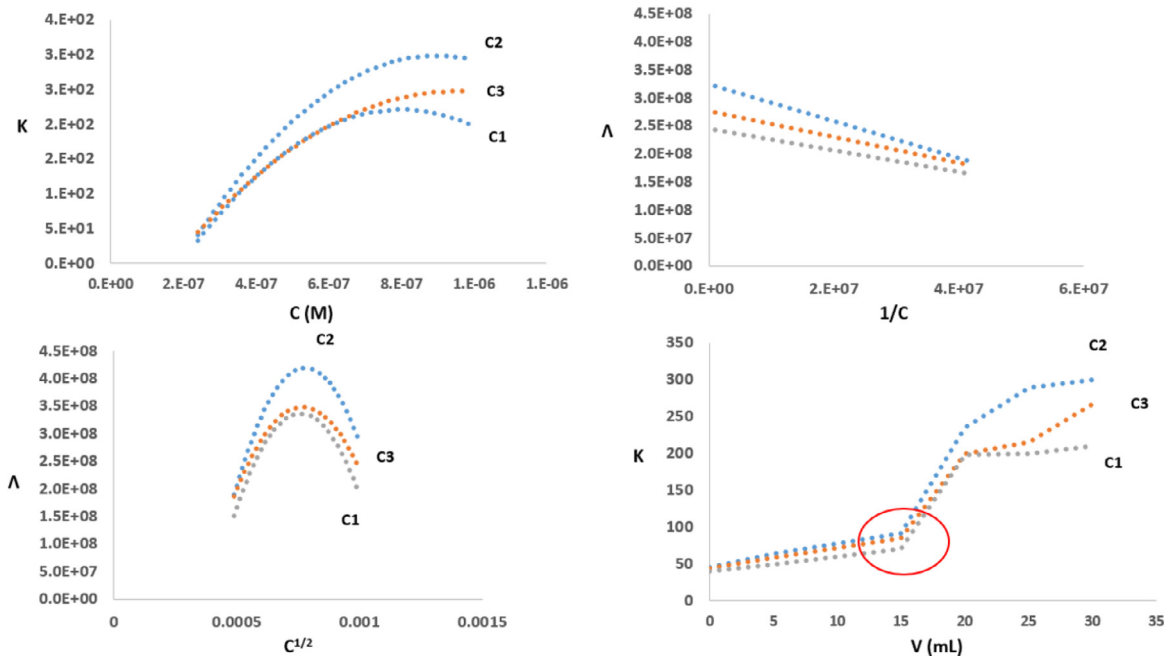

Fig. 9. Conductivity graphs of the interactions between the Zn(II)-complexes and BSA.

drastic change in the spectrum was happened by the complexed C_1, C_2, C_3 molecules. Additionally, the results indicated that the interaction of the Zn (II) complexed chalcones with BSA molecule has caused some conformational changes in the microenvironment around chromophore of BSA, that is why we cannot observe any peak at the 300 nm.

Conductance studies on the Zn-complexes interaction with BSA

The values of molar conductivity Λ (s m^2 mol^{-1}) in corelation of the $\sqrt{C}$ are shown in Fig. 9. In the same figure we can see the conductivity K ($\mu s/cm^2$) values in corelation with the added volume of the zinc derivative to the BSA. On this graph it is significant the change of the slope of the plot which corresponds to the protein-ligand complex formation. Based on the graph of the molar conductivity versus 1/C we were able to calculate the binding constants K_b (M^{-1}) of the complexes. The sigmoid curve allows to calculate for the binding constant (K_b) in the following manner. Assuming that a free Zinc complex molecule (S) and a free protein (D) form 1:1 complex (X), K_b is expressed as $K=C_X/C_S{}^*C_D$ whereas C corresponds to their concentrations.

It seems that C_1 molecule has the higher binding constant (0.51), followed by C_3 (0.43) and then by C_2 (0.30). these results are in agreement both with the results taken by the UV-vis spectroscopy and the theoretical ones taken by the molecular docking studies. Again here, the two methyl groups that C_2, has were responsible for the increase of the van der Waals interactions of the molecule with the binding site of the protein [41].

4. Conclusions

In this work, the synthesis of three chalcone derivatives and their corresponding Zn (II) molecules was presented and their structures evaluated spectroscopically and theoretically. Their spectroscopic and theoretical evaluation indicated that the Zn-chalcone molecules exhibited higher binding activity than their corresponding chalcone ligands. The binding activity was predicted with molecular docking studies and confirmed by spectroscopic BSA interactions of **L_1, L_2, L_3, C_1, C_2** and **C_3**. From the highest to lowest activity the molecules are **C_2>C_3>L_3>C_1>L_1>L_2**. Chalcones are biological active molecules and their interactions with Zn metal ion increases their binding activity on transport proteins. Additionally, these chalcone derivatives could be used in a study as biological chelators to reduce the toxic zinc concentrations in biological systems.

Declaration of competing interest

The author declares that they have no known competing financial interests or personal relationships that could have appeared to influence the work reported in this paper.

Acknowledgements

The author wants to acknowledge the Pharmacy Programme of the University of Nicosia and Dr. Demetris Apostolides of the Department of Chemistry, of the University of Cyprus for the NMR experiments.

References

[1] S Verma, AK Srivastava, OP Pandey, A Review on Chalcones Synthesis and their Biological Activity, PharmaTutor 6 (2) (2018) 22–39 10.29161/PT.v6.i2.2018.22.
[2] M. Asad, M. Arshad, S. Khan, M. Oves, M. Khalid, A. Asiri, et al., Cyclization of chalcones into N-propionyl pyrazolines for their single crystal X-ray, computational and antibacterial studies, Journal Of Molecular Structure 1201 (2020) 127186, doi:10.1016/j.molstruc.2019.127186.
[3] S.W. Khor, Y.K. Lee, M.R.B. Abas, et al., Application of chalcone-based dithiocarbamate derivative incorporated sol–gel for the removal of Hg (II) ion from water, J Sol-Gel Sci Technol 82 (2017) 834–845, doi:10.1007/s10971-017-4362-7.
[4] R. Kamal, R. Kumar, V. Kumar, V. Bhardwaj, Synthetic Utilization of α,β-Chalcone Dibromide In Heterocyclic Chemistry and Stereoselective Debromination, Chemistryselect 4 (2019) 11578–11603, doi:10.1002/slct.201902262.
[5] Xu Zhanga, K.P. Rakesha, S.N.A. Bukharia, Moku Balakrishnaa, H.M. Manukumarb, Hua-Li Qina, Multi-targetable chalcone analogs to treat deadly Alzheimer's disease: Current view and upcoming advice, Bioorganic Chemistry 80 (2018) 86–93.
[6] Ayse Aktas Kamiloglu, Hüseyin Karaca, Gonca Celik, Irfan Acar, Halit Kantekin, New chalcone-substituted metallophthalocyanines: Synthesis, characterization, and investigation of their properties, Journal of Chemical Research (2020) 1–10 https://journals.sagepub.com/doi/10.1177/1747519820902684.
[7] Mohamed Gabera, Hoda A. El-Ghamrya, Mohammed A. Mansourc, Pd(II) and Pt(II) chalcone complexes. Synthesis, spectral characterization, molecular modelling, biomolecular docking, antimicrobial and antitumor activities, Journal of Photochemistry and Photobiology A: Chemistry 354 (2018) 163–174.
[8] Gülpınar Sarkı, Halit Kantekin, Halise Yalazan, Nuran Kahriman, Zekeriya Biyiklioglu, Vildan Serdaroglu, Synthesis, characterization and electrochemical studies of metal-free and metallophthalocyanines containing two different chalcone units substituted on peripherally positions, Journal of Molecular Structure 1196 (2019) 592e603.
[9] Chiara Sulpizio, Joscha Breibeck, Annette Rompel, Recent progress in synthesis and characterization of metal chalcone complexes and their potential as bioactive agents, Coordination Chemistry Reviews 374 (2018) 497–524.
[10] Mohammed Rayees Ahmad, V.Girija Sastry, Nasreen Bano, Syed Anwar, Synthesis of novel chalcone derivatives by conventional and microwave irradiation methods and their pharmacological activities, Arabian Journal of Chemistry 9 (2016) S931–S935.
[11] Mohammad Azam, Saud.I. Al-Resayes, Raghavaiah Pallepogu, Farha Firdaus, Mohammad Shakir, Mononuclear Bis(3-aminoquinoline)Zn(II) complexes: Synthesis and structural characterization, Journal of Saudi Chemical Society 20 (2016) 120–126.
[12] Artur Krezel, Wolfgang Maret, The biological inorganic chemistry of zinc ion, Archives of Biochemistry and Biophysics 611 (2016) 3e19.4.
[13] Long Fan, Jing-can Qin, Chao-rui Li, Zheng-yin Yang, Two similar Schiff-base receptor based quinoline derivate: Highly selective fluorescent probe for Zn(II), Spectrochimica Acta Part A: Molecular and Biomolecular Spectroscopy (2018), doi:10.1016/j.saa.2020.118347.
[14] Chenxiang Wang, Dawei Shi, Fangfang Zhang, Xuben Yu, Guanyang Lin, Ziye Zhou, Characterization of binding interaction between magnesium isoglycyrrhizinate and human serum albumin, Spectrochimica Acta Part A: Molecular and Biomolecular Spectroscopy 234 (2020) 118245.
[15] Ankita Varshney, Priyankar Sen, Ejaz Ahmad, Mohd. Rehan, Naidu Subbarao, Rizwan Hasan Khan, Ligand Binding Strategies of Human Serum Albumin: How Can the Cargo be Utilized? CHIRALITY 22 (2010) 77–87.
[16] Rachana Srivastava, Md. Sayem Alama, Spectroscopic studies of the aggregation behavior of Human Serum Albumin and cetyltrimethylammonium bromide, International Journal of Biological Macromolecules 158 (2020) 394–400.
[17] Tanveer A. Wani, Ahmed H. Bakheit, M. A. Abounassif and Seema Zargar, Study of Interactions of an Anticancer Drug Neratinib With Bovine Serum Albumin: Spectroscopic and Molecular Docking Approach, Front. Chem. 6:47. doi: 10.3389/fchem.2018.00047.
[18] Fang Shen, Ya-Xian Liu, Shu-Min Li, Chi-Kun Jiang, Bing-Feng Wang, Ya-Hong Xiong, Zong-Wan Mao, Xue-Yi Le, Synthesis, crystal structures, molecular docking and in vitro cytotoxicity studies of two new copper (II) complexes: special emphasis on their binding to HAS, NewJ.Chem 41 (2017) 12429.
[19] Serpil Kaya, Sultan Erkan, Duran Karakaş, Computational investigation of molecular structures, spectroscopic properties and antitumor-antibacterial activities of some Schiff bases, Spectrochimica Acta Part A: Molecular and Biomolecular Spectroscopy 244 (2021) 118829.
[20] Prateek Tyagi, Sulekh Chandra, B.S. Saraswat b, Deepansh Sharma, Design, spectral characterization, DFT and biological studies of transition metal complexes of Schiff base derived from 2-aminobenzamide, pyrrole and furan aldehyde, Spectrochimica Acta Part A: Molecular and Biomolecular Spectroscopy 143 (2015) 1–11.
[21] Gao-Jun Zhang, Shao-Yi Wu, Chen-Hao Liang, Yi-Mei Fan, Ying-Jie Luo, Jia-Xing Guo, Xiao-Yu Li, DFT calculations of the local structures and the EPR parameters for Rh2+ doped AO (A = Mg, Ca) crystals, Chemical Physics 534 (2020) 110734.
[22] G. Kirishnamaline, J. Daisy Magdaline, T. Chithambarathanu, D. Aruldhas, A. Ronaldo Anuf, Theoretical investigation of structure, anticancer activity and molecular docking of thiourea derivatives, Journal of Molecular Structure 1225 (2021) 129118.
[23] M.K. Tripathi, P. Sharma, A. Tripathi, et al., Computational exploration and experimental validation to identify a dual inhibitor of cholinesterase and amyloid-beta for the treatment of Alzheimer's disease, J Comput Aided Mol Des 34 (2020) 983–1002.
[24] J. Hu, C. Yan, A tool for calculating binding-site residues on proteins from PDB structures, BMC Struct Biol 9 (2009) 52, doi:10.1186/1472-6807-9-52.
[25] Jingwei Zhou, Min Li, Nanhao Chen, Shenglong Wang, Hai-Bin Luo, Yingkai Zhang, Ruibo Wu, Computational Design of a Time-Dependent Histone Deacetylase 2 Selective Inhibitor, ACS Chem. Biol. 10 (2015) 687–692.
[26] S. Syed Ali Fathima, M.Mohamed Sahul Meeran, E.R. Nagarajana, Synthesis of novel (E)-2-((anthracen-9-ylmethylene) amino) pyridin-3-ol and its transition metal complexes: Multispectral characterization, biological evaluation and computational studies, Journal of Molecular Liquids 279 (2019) 177–189.
[27] R.N.S. Santiagoa, P.T.C. Freirea, A.M.R. Teixeirac, P.N. Bandeirae, H.S. Santose, T L.G. Lemosf, C.A.N. Ferrazc, FT-Raman and FT-IR spectra and DFT calculations of chalcone (2E)-1-(4-aminophenyl)-3-phenyl-prop-2-en-1-one, Vibrational Spectroscopy 97 (2018) 1–7.
[28] Shui Wang, Qiaoli He, Jidong Wang, Yixin Qu, Molecular structural, IR and NMR spectroscopic studies on the four isomers of thiotriazinone by DFT and HF calculations, Spectrochimica Acta Part A 87 (2012) 179–189.
[29] Sudhir M. Hiremath, Seema S. Khemalapure, Chidanandayya S.Hiremath b, Anil S. Pati, Mahantesha Basanagouda, Quantum chemical computational and spectroscopic (IR, Raman, NMR, and UV) studies on the 5-(5-methoxy-benzofuran-3-ylmethyl)- 3H-[1, 3, 4] oxadiazole-2-thione, Journal of Molecular Structure 1210 (2020) 128041.
[30] Parutagouda Shankaragouda Patil, Neelamma B. Gummagol, Anusha Ekbote, Qin AiWong, Ching Kheng Quah, Mohd Shkir, Shivaraj R. Maidur, S. Venugopal Rao, Journal of Molecular Structure 1219 (2020) 128523.
[31] Chandra Kereyagalahally Honneshappa Narasimhamurthy, Toreshettahally Ramesh Swaroop, Swamy Jagadish, Kanchugarakoppal Subbegowda Rangappa, Synthesis of Piperidine Conjugated Dihydroquinazolin-4(1H)-ones and their Antiproliferative Activity, Molecular Docking Studies and DFT Calculations, Letters in Drug Design & Discovery 17 (2020) 85–93.
[32] Ajay Kumar, Kamlesh Kumari, Indra Bahadur, Prashant Singh, Temperature dependent DFT studies to understand the physiochemical interaction of lithium chloride cluster ions in presence of syringic acid, J. Chem. Thermodynamics 152 (2021) 106277.
[33] Bao-Li Wang, Dong-Qi Pan, Song-Bo Kou, Zhen-Yi Lin, Jie-Hua Shi, Exploring the binding interaction between bovine serum albumin and perindopril as well as influence of metal ions using multi-spectroscopic, molecular docking and DFT calculation, Chemical Physics 530 (2020) 110641.
[34] Sudhir M. Hiremath, A. Suvitha, Ninganagouda R. Patil, Chidanandayya S. Hiremath, Seema S. Khemalapure, Subrat K. Pattanayak, Veerabhadrayya S. Negalurmath, Kotresh Obelannavar, Molecular structure, vibrational spectra, NMR, UV, NBO, NLO, HOMO-LUMO and molecular docking of 2-(4, 6-dimethyl-1-benzofuran-3-yl) acetic acid (2DBAA): Experimental and theoretical approach, Journal of Molecular Structure 1171 (2018) 362e374.

[35] Nazia Siddiqui, Saleem Javed, Quantum computational, spectroscopic investigations on ampyra (4-aminopyridine) by df t/td-df t with different solvents and molecular docking studies, Journal of Molecular Structure 1224 (2021) 129021.
[36] Julian Tirado-Rives, William L. Jorgensen, Performance of B3LYP Density Functional Methods for a Large Set of Organic Molecules, J. Chem. Theory Comput. 4 (2008) 297–306.
[37] T.R. Garcia, T.S. de Freitas, H.S. dos Santos, P.N. Bandeira, M.S.S. Juli~ao, J.E. Rocha, C.E.S. Nogueira, R.L.S. Pereira, A.C.H. Barreto, P.T.C. Freire, H.D.M. Coutinho A.M.R. Teixeira, Structural, vibrational and electrochemical analysis and antibiotic activity study of chalcone (2E)-1-(3′,-methoxy-4′,-hydroxyphenyl)-3- (3-nitrophenyl)prop-2-en-1-one, Journal of Molecular Structure 1216 (2020) 128358.
[38] Serdal Kaya, Halil Gokce, Tayfun Arslan, Gokhan Alpaslan, Synthesis, spectroscopic characterization, DFT computations, nonlinear optical profile and molecular docking study of a novel chalcone derivative, Journal of Molecular Structure 1202 (2020) 127270.
[39] Amit Kumar, Rajesh Kumar, Archana Gupta, Poonam Tandon, E. Deepak D'silva, Molecular structure, nonlinear optical studies and spectroscopic analysis of chalcone derivative (2E)-3-[4-(methylsulfanyl) phenyl]- 1-(3-bromophenyl) prop-2-en-1-one by DFT calculations, Journal of Molecular Structure 1150 (2017) 166e178.
[40] Tiyas Pal, Pooja Patil, Abha Sharma, Synthesis, molecular docking and spectroscopic studies of pyridoxine carbamates as metal chelator, Journal of Molecular Structure 1223 (2021) 128837.
[41] M. Manabe, H. Kawamura, H. Katuura, M. Shiomi, The Application of Differential Conductivity Method to the Determination of Binding Constant of β-Cyclodextrin with Sodium Perfluorooctanoate, in: J.J.T. Labandeira, J.L. Vila-Jato (Eds.), Proceedings of the Ninth International Symposium on Cyclodextrins, Springer, Dordrecht, 1999, doi:10.1007/978-94-011-4681-4_154.